

1. Introduction

Light absorbing carbon (LAC) is the fraction of carbonaceous aerosol, which can absorb electromagnetic radiation in the visible or near-visible range (Pöschl, 2003; Bond and Bergstrom, 2006; Moosmüller et al., 2009; Ferrero et al., 2018). A wide literature investigates and characterizes the optical properties of the inorganic-refractory LAC fraction, usually referred as Black Carbon, BC, (e.g., Bond et al., 2013; and references therein) which is strongly absorbing from UV to IR, with a weak dependence on wavelength (Bond and Bergstrom, 2006; Moosmüller et al., 2009). Much less studied and understood is the organic LAC, often labelled as Brown Carbon (BrC), which appears to be optically active at wavelengths shorter than 650 nm and with an increasing absorbance moving to the blue and ultraviolet (UV) range (Pöschl, 2003; Andreae and Gelencsér, 2006; Moosmüller et al., 2011; Laskin et al., 2015; Olson et al., 2015). BrC can therefore be considered as the “optically active” part of the OC dispersed in the atmosphere. When considered from a thermo-chemical point of view, BrC also shows a refractory behaviour since, in an inert atmosphere, it volatilizes at temperatures greater than 400 °C only (Chow et al., 2015). A discussion on the primary and secondary sources of atmospheric LAC is outside the scope of the present work; we simply remind that primary BrC is produced mainly by biomass burning even if, in some cases, also incomplete combustion of fossil fuels used in transport activities (i.e., terrestrial vehicles, ships and aircrafts) can generate this kind of compounds (Corbin et al, 2018). It is also worth to underline that carbonaceous aerosols impact on human health (Pope and Dockery, 2006; Chow et al., 2006; Mauderly and Chow, 2008), as well as on climate and environment (Bond and Sun, 2005; Highwood and Kinnersley, 2006; Chow et. al., 2010).

In the wider landscape of atmospheric carbonaceous aerosol, despite a worldwide diffused effort, the situation is not satisfactory and a standardized and conclusive approach is still missing. The quantitative determination of total, organic and elemental carbon (TC, OC and EC) is often performed by a thermal-optical analysis (Birch and Cary, 1996; Watson et al., 2005; Hitzenberger et al., 2006) of aerosol samples collected on quartz fibre filters. However, thermal-optical analyses are affected by several issues and artefacts (Yang and Yu, 2002; Chow et al., 2004) and different laboratories/agencies adopt protocols which systematically result in discrepancies, particularly large in the EC quantification (Birch and Cary, 1996; Chow et al., 2007; Cavalli et al., 2010). A further issue arises when the effects of the possible presence of BrC in the sample are taken into account. So far, the monitoring of the sample transmittance during the thermal cycle, has been introduced to correct for the well-know charring effect and

71 the formation of pyrolytic carbon (Birch and Cary, 1996). This implies that BC is the sole
72 absorbing compound at the wavelength implemented in the thermal-optical analyser (for
73 instance at $\lambda = 635$ nm, the wavelength of the laser diode mounted in the extremely diffused
74 Sunset Lab. Inc. EC/OC analyzer). Basically, with a sizeable concentration of BrC in the
75 sample, one of the key assumptions of the thermal-optical methods fails and the EC/OC
76 separation is even more unstable (not to say that, by design, the BrC quantification is not
77 possible). This issue was preliminarily addressed by (Chen et al., 2015) by a multi-wavelength
78 thermal-optical reflectance/thermal-optical transmittance (TOR/TOT) instrument (Thermal
79 Spectral Analysis – TSA) and further investigated in (Massabò et al., 2016). In the latter work,
80 a method to correct the results of a standard Sunset analyzer and to retrieve the BrC
81 concentration in the sample was introduced. The achievement was possible thanks to a synergy
82 with the information provided by the Multi Wavelength Absorbance Analyzer, MWAA,
83 (Massabò et al., 2015) developed in the same laboratory. A further step towards BrC
84 quantification through the utilization of TSA was discussed in (Chow et al., 2018), where it
85 was proved that the use of 7 wavelengths in thermal-optical carbon analysis allows
86 contributions from biomass burning and secondary organic aerosols to be estimated. It is
87 worthy to note that the biomass burning contribution to PM concentration can also be estimated
88 by other methods such as Aerosol Mass Spectrometry, AMS (Daellenbach et al., 2016).

89 The MWAA approach allows the determination of the spectral dependence of the aerosol
90 absorption coefficient (b_{abs}) which can be generally described by the power-law relationship
91 $b_{\text{abs}}(\lambda) \sim \lambda^{-\text{AAE}}$, where the AAE is the Ångström Absorption Exponent. Several works reported
92 AAE values which depend on the aerosol chemical composition (Kirchstetter et al., 2004; Utry
93 et al., 2013) as well as its size and morphology (Lewis et al., 2008; Lack et al., 2012; Lack and
94 Langridge, 2013; Filep et al., 2013; Utry et al., 2014). Furthermore, the spectral dependence of
95 the aerosol has been exploited to identify different sources of carbonaceous aerosol (e.g.,
96 Sandradewi et al., 2008; Favez et al., 2010; Lack and Langridge, 2013; Massabò et al., 2013
97 and 2015). In general, AAE values close to 1.0 have been found to be related to urban PM
98 where fossil fuels combustion is dominant, while higher AAE values, up to 2.5, have been
99 linked to carbonaceous aerosols produced by wood burning (Harrison et al., 2013; and
100 references therein) and therefore to the presence of BrC.

101 In the previous work by (Massabò et al., 2016) the effect of the BrC possibly contained in
102 the sample on the thermal-optical analysis was quantified and exploited to retrieve the BrC
103 concentration from the raw data provided by a standard Sunset Lab. Analyzer. This first step,

104 suggested to modify/upgrade a Sunset unit adding the possibility to use a second laser diode in
105 the blue range. This improves the sensitivity to the BrC and allows to check whether the BrC
106 quantification depends on the adopted wavelength. We finally followed this route and we here
107 introduce our modified Sunset Analyzer unit, the validation tests and the results of the first
108 campaign in which the new unit was deployed.

109

110 **2. Materials and Methods**

111

112 **2.1 The 2-lambda SUNSET analyzer**

113 We have modified a commercial Thermal Optical Transmittance (TOT) instrument (Sunset
114 Lab Inc.). This equipment had been originally designed (Birch and Cary, 1996) with a red laser
115 diode ($\lambda = 635$ nm) to have the possibility to monitor and correct the well-know problem of
116 the formation of pyrolytic carbon by charring (Birch and Cary, 1996; Bond and Bergstrom,
117 2006; Chow et al., 2007; Cavalli et al., 2010). The assumption that OC is optically inactive at
118 wavelengths greater than 600 nm is at the basis of the technique; therefore the laser beam
119 attenuation is only due to the EC originally present or formed by charring in the sample under
120 analysis. Actually, even at this wavelength, BrC can affect the reliability of the OC/EC
121 separation and the standard methodology can be modified to quantify the BrC concentration
122 (Massabò et al., 2016). Nevertheless, at $\lambda = 635$ nm the BrC Mass Absorption Coefficient,
123 MAC(BrC), remains much smaller than the corresponding MAC(BC) and the modified
124 procedure could/should be implemented at shorter wavelengths to gain in sensitivity.

125 We have modified our SUNSET unit making possible the alternative use of the standard
126 laser diode at $\lambda = 635$ nm or of a World Star Technologies, 100 mW, laser diode at $\lambda = 405$
127 nm. This second laser diode can be mounted on the top of the SUNSET furnace by a homemade
128 adapter (see Figure 1) and easily exchanged with the native red diode. With the new laser
129 diode, the light detector placed at the bottom of the SUNSET furnace has to be changed too
130 and we selected a photodiode (PD) THORLABS FDS1010 coupled with a bandpass filter
131 THORLABS FBH405-10. The responsivity of the PD FDS1010 around $\lambda = 400$ nm is quite
132 low (about 50 mA W^{-1}) but the high power delivered by the laser diode results in signals with
133 an amplitude comparable to the values measured with the original SUNSET set-up (i.e., laser
134 diode and PD). Furthermore, the FBH405-10 filter cuts all the light background produced by
135 the high temperature of the SUNSET furnace, thus preserving the signal-to-noise ratio. Both
136 laser and PD can be exchanged in about 10 min and no particular attention is requested but the

137 proper alignment to maximize the PD output signal (i.e., the *transmittance* value displayed by
138 the SUNSET control software). We have to note that the original configuration of the SUNSET
139 instrument adopts a lock-in amplifier to improve the signal-to-noise ratio of the PD: we did not
140 have the possibility to manipulate the parameters of the lock-in amplifier and to tune it to the
141 new configuration.

142

143 **2.2 Test of the new configuration**

144 The new blue-light set-up of the Sunset Analyzer was tested using both synthetic and real-
145 world aerosol samples, collected on quartz fibre filters. Synthetic samples were prepared
146 starting with a 5% (volume) solution of Aquadag, then nebulised by a Blaustein Atomizer
147 (BLAM) and collected on quartz fibre filters. Aquadag is the trade name of a water-based
148 colloidal graphite coating (particle diameters between 50 and 100 nm): these samples can
149 therefore be considered to be composed of EC/BC only. The samples were first sent to an
150 optical characterization by the MWAA instrument (Massabò et al., 2015) which demonstrated
151 that the optical absorption of Aquadag is independent on the wavelength. Actually, Aquadag
152 particles tend to form conglomerates on the filter surface, with dimension about double of the
153 longer wavelength implemented in the MWAA (i.e., the 850 nm of the infrared laser diode;
154 Massabò et al., 2015). So, the comparison between the new blue-light and original Sunset set-
155 ups was made with samples having the same absorption properties. EC and TC quantifications
156 obtained at $\lambda = 635$ nm and $\lambda = 405$ nm were in excellent agreement for both the NIOSH5040
157 and EUSAAR_2 protocol (Cavalli et al., 2010), as shown in Figure 2 for the whole set of
158 synthetic samples.

159 A second set of synthetic samples was prepared to mimic the behaviour of real-world aerosol
160 samples: a 3% (weight) solution of ammonium sulphate $(\text{NH}_4)_2\text{SO}_4$ in Aquadag was prepared
161 and nebulized with the BLAM. This way, a scattering compound is mixed to the absorbing
162 Aquadag spherules. The optical absorption measured with MWAA was independent on
163 wavelength with this second set of samples too. The results of the Sunset analysis with both
164 the red and blue laser set-up are shown in Figure 3. This second set of samples was analysed
165 through the EUSAAR_2 protocol only: we used two punches for each laser in each sample to
166 have a reproducibility check. A strong correlation between the TC and EC values measured in
167 red and blue light was obtained again with a slope close to unity.

168 A third and final test was performed using a set of daily PM10 samples collected by a low-
169 volume sampler (TCR - Tecora, Italy) on quartz fibre filters (Pall-2500 QAO-UP, 47 mm
170 diameter) in spring 2016 in the urban area of the city of Genoa (Italy). A previous and long set

171 of similar campaigns addressed to PM10 characterization (e.g., Bove et al., 2014 and references
172 therein) in the same urban area could not identify a sizeable contribution from biomass burning
173 to PM composition, in particular during spring and summer. Such situation was confirmed by
174 the determination of the Ångström exponent in the present samples by the MWAA. Actually,
175 in the set of twenty PM10 samples, the values of the Ångström exponent ranged between 0.9
176 and 1.2, this confirming that Black Carbon is the sole or totally dominant light absorbing
177 component in the local PM10 (Sandradewi et al., 2008; Harrison et al., 2013). Half of the
178 samples was then sent to the Sunset analysis by the NIOSH5040 protocol while the
179 EUSAAR_2 protocol was adopted for the remaining subset. The results are shown in Figure 4.
180 The EC concentration values measured with the standard and modified Sunset analyzer are
181 fully compatible when the NIOSH5040 protocol is adopted (basically, the split point position
182 in the Sunset thermogram does not change with the two laser diodes). Instead, EC values
183 determined by the EUSAAR_2 protocol resulted in about 30% lower values when the blue
184 laser diode was mounted. This corresponds to a shift of the split point position, which moves
185 rightward and thus increases the amount of carbonaceous aerosol counted in the OC fraction.
186 This effect is linked to the well-known issue of the formation of pyrolytic carbon during the
187 thermal cycle in the inert atmosphere (i.e., in He). Several literature studies (e.g., Cavalli et al.,
188 2010; Panteliadis et al., 2015) indicated that the charring is smaller at the higher temperatures
189 reached during the NIOSH thermal protocol. On the other way, standard thermal-optical
190 analyses of urban PM samples often give higher EC values (up to 50%) when performed
191 following the EUSAAR_2 instead of higher-temperature protocols (Subramanian et al., 2006;
192 Zhi et al., 2008; Piazzalunga et al., 2011; Karanasiou et al., 2015; Panteliadis et al., 2015).
193 Furthermore, as by-product of previous PM10 studies in the urban area of Genoa by a standard
194 Sunset unit, we could observe a systematic and very reproducible 40% discrepancy between
195 EC values determined in the same samples by EUSAAR_2 and NIOSH5040 protocols (with
196 EC: EUSAAR > EC: NIOSH). Therefore, the thermal-optical analysis in blue light seems to
197 be more sensitive to the charring formation during the EUSAAR_2 protocol.

198

199 **3. First field campaign and results**

200

201 The modified Sunset instrument was used for the first time, in conjunction with the MWAA
202 instrument and apportionment methodology (Massabò et al., 2015), to retrieve the MAC (Mass
203 Absorption Coefficient) of Brown Carbon at the two wavelengths of $\lambda = 635$ nm and $\lambda = 405$
204 nm, in a set of samples collected during wintertime in a mountain site.

205

206 **3.1 Samples collection**

207 Aerosol samples were collected in a small village (Propata, 44°33'52.93''N, 9°11'05.57''E,
208 970 m a.s.l.) situated in the Ligurian Apennines, Italy. Three different sets of PM10 aerosol
209 samples were collected by a low-volume sampler (38.3 l min⁻¹ by TCR Tecora): the first and
210 the third sets had filter change set every 24h while the second set was sampled on a 48h-basis.
211 In total, 41 (14+13+14) PM10 samples were collected on quartz-fibre filters (Pall, 2500QAO-
212 UP, 47 mm diameter), between February 2nd and April 19th, 2018. Before the sampling, the
213 filters were baked at T = 700°C for 2 hours to remove possible internal contamination. Field
214 blank filters were used to monitor possible contaminations during the sampling phase. Wood
215 burning is one of the PM sources around the sampling site, especially during the cold season,
216 as it is used for both domestic heating and cooking purposes.

217

218 **3.2 Laboratory analyses**

219 All filters were weighed before and after sampling in an air-conditioned room (T = 20 ± 1
220 °C; R.H. = 50 % ± 5%), after 48h conditioning. The gravimetric determination of the PM mass
221 was performed using an analytical microbalance (precision: 1 µg) which was operated inside
222 the conditioned room; electrostatic effects were avoided by the use of a de-ionizing gun.

223 After weighing, samples were first optically analyzed by MWAA to retrieve the absorption
224 coefficient (b_{abs}) of PM at five different wavelengths. The EC and OC determination was
225 performed adopting the EUSAAR_2 protocol (Cavalli et al., 2010) with both laser diodes at λ
226 = 635 nm and at $\lambda = 405$ nm (two different punches were extracted from each filter sample).

227 Finally, the remaining portion of the same quartz-fibre filters underwent a chemical
228 determination of the Levoglucosan (1,6-Anhydro-beta-glucopyranose) concentration by High
229 Performance Anion Exchange Chromatography coupled with Pulsed Amperometric Detection
230 (Piazzalunga et al., 2010). As well-known in literature, this sugar is one of the typical markers
231 of biomass burning (Vassura et al., 2014).

232

233 **3.3 Optical apportionment**

234 The MWAA analysis provided the raw data to measure the spectral dependence of the
235 aerosol absorption coefficient (b_{abs}) which can be generally described by the power-law
236 relationship $b_{\text{abs}}(\lambda) \sim \lambda^{-\text{AAE}}$ where AAE is the Ångström Absorption Exponent.

237 The time series of the resulting AAE values is shown in Figure 5: they range between
238 1.05 and 1.96 with a mean value of 1.55 ± 0.21 . This figure indicates a substantial presence of
239 wood burning in the sampling area. In (Massabò et al., 2015 and Bernardoni et al, 2017), an
240 optical apportionment model (the “MWAA model”) based on the measurement of b_{abs} at five
241 wavelengths had been introduced to obtain directly the BrC AAE (α_{BrC}) and the BrC absorption
242 coefficient ($b_{\text{abs}}^{\text{BrC}}$) at each measured wavelength. It is worthy to note that, at the basis of the
243 MWAA model, there is the assumption that BrC is produced by wood combustion only (see
244 §4 in Massabò et al., 2015; Zheng et al., 2013). In Figure 5, we report the optical apportionment
245 at $\lambda = 635$ nm and at $\lambda = 405$ nm, i.e., at the wavelength of the two laser diodes used in our
246 modified Sunset instrument. At $\lambda = 635$ nm, light absorption resulted mainly due to BC from
247 both fossil fuel (FF) and wood burning (WB) and the $b_{\text{abs}}^{\text{BrC}}$ average value is 15% of total b_{abs} ,
248 with the notable exception of some days in which it reached values of $\sim 30\%$, in
249 correspondence of $\text{AAE} > 1.9$. Instead, at $\lambda = 405$ nm, the BrC contribution to light absorption
250 rises up to 33% (average percentage of total b_{abs}), with a maximum value of 51%, again when
251 $\text{AAE}_{\text{exp}} > 1.9$. The time series of $b_{\text{abs}}^{\text{BrC}}$ values at both wavelengths turned out to be well
252 correlated ($R^2 = 0.71$) with the Levoglucosan (*Levo*, in the following) concentration values, as
253 reported in Figure 6. The slope of the correlation curve increases by a factor 5.8 when moving
254 from the red to the blue light.

255 The average α_{BrC} value turned out to be $\alpha_{\text{BrC}} = 3.9 \pm 0.1$, in very good agreement with a
256 previous value ($\alpha_{\text{BrC}} = 3.8 \pm 0.2$) obtained in the same site and with the same approach
257 (Massabò et al., 2016). The result is also in agreement with other literature works (Yang et al.,
258 2009; Massabò et al., 2015; Chen et al., 2015).

259

260 **3.4 Brown Carbon MAC**

261 The methodology to extract the MAC value for BrC by the coupled use of MWAA and
262 thermal-optical analysis has been introduced in a previous work (Massabò et al., 2016). In that
263 case, a standard (i.e., with a red laser diode only) a Sunset unit was used. The entire procedure
264 is described in details in (Massabò et al., 2016), here we briefly summarize the main steps:

- 265 a) The fraction of light attenuation due to the BrC is first calculated in each sample with
266 the MWAA raw data.
- 267 b) The empirical relationship between the light attenuation through the sample, observed
268 in the MWAA and in the Sunset and at both wavelengths, is then determined. We remind
269 that in the Sunset measurement, the light attenuation is continuously recorded during

270 the analysis; the value characteristic of each blank filter can be retrieved when all the
271 light absorbing PM has been volatilized (i.e., at the end of the thermal protocol).

272 c) The fraction of light attenuation due to the BrC in the sample is therefore calculated for
273 the Sunset analysis and the initial transmittance value is corrected to estimate the
274 attenuation value that it would have been found if BrC were not present in the filter
275 sample.

276 d) A new split-point position is then determined taking into account the corrected value of
277 the initial transmittance.

278 e) The OC and EC values determined with the standard and corrected split-point positions
279 are then compared and the difference ($OC_{cor} - OC_{std} = EC_{std} - EC_{cor}$) is operatively
280 assumed to be equal to the BrC in the sample. The corresponding BrC atmospheric
281 concentration is finally calculated.

282 f) The correlation between the values of b_{abs}^{BrC} , provided by the MWAA analysis (see
283 section 3.3) and BrC concentration, is studied to determine the MAC value.

284

285 In the present experiment, the procedure was adopted to analyse the thermograms produced
286 with both the red and the blue laser diode mounted in the Sunset unit: the results are
287 summarized in Figure 7. Despite a rather high noise in the data, the MAC(BrC) value at the
288 two wavelengths can be determined and it turns out to be $MAC(BrC) = 9.8 \pm 0.4 \text{ m}^2 \text{ g}^{-1}$ and 23
289 $\pm 1 \text{ m}^2 \text{ g}^{-1}$, respectively at $\lambda = 635$ and 405 nm . This result deserves some comments:

290 • The MAC value at $\lambda = 635 \text{ nm}$ differs for about 3σ from the result reported in (Massabò
291 et al., 2016) and obtained for the same site and in a similar season (i.e., November 2015
292 to January 2016; $MAC = 7.0 \pm 0.4 \text{ m}^2 \text{ g}^{-1}$). Since differences in the type of wood burnt
293 in the past and present campaign cannot be excluded, the two values can be considered
294 to be in fair agreement.

295 • No comparison with previous or other literature values is possible for the MAC value
296 at $\lambda = 405 \text{ nm}$, given the substantial differences in adopted definitions and
297 methodologies (Yang et al., 2009; Feng et al., 2013; Chen and Bond, 2010). However,
298 the increase by a factor 2.3 with respect to the MAC at $\lambda = 635 \text{ nm}$ follows the expected
299 behaviour.

300 • Under the assumption that the sole source of BrC is biomass burning, the MAC values
301 can be referred to the total concentration of organic carbon (i.e., including the part not
302 optically active) produced by biomass burning. Adopting with the present data set the

303 optical OC apportionment methodology reported in (Massabò et al., 2015), the BrC
304 values determined at $\lambda = 635$ nm turn out to be about 4% of the OC produced by wood
305 combustion, OC_{WB} , and consequently $MAC(OC_{WB}, \lambda = 635\text{nm}) = 0.39 \pm 0.06 \text{ m}^2 \text{ g}^{-1}$.
306 When the analysis is performed at $\lambda = 405$ nm, BrC results to be about 10% of OC_{WB}
307 and $MAC(OC_{WB}, \lambda = 405\text{nm}) = 2.3 \pm 0.2 \text{ m}^2 \text{ g}^{-1}$. Previous literature works (Feng et al.,
308 2013; Laskin et al., 2015; and references therein) report MAC values of BrC and/or
309 related OC ranging in a quite large interval.

- 310 • The ratio between BrC and Levo concentration values results to be $BrC:Levo = 0.19 \pm$
311 0.02 and 0.42 ± 0.06 , respectively when considering the BrC concentration determined
312 by MWAA + Sunset at $\lambda = 635$ and 405 nm. In other words, the operative procedure,
313 introduced in (Massabò et al., 2016), results in different BrC concentration values
314 according to the considered/used wavelength. This fact can be interpreted in different
315 ways: while the analytical sensitivity is higher at $\lambda = 405$ nm and the corresponding
316 BrC values could be considered to be more firm, the category of compounds collected
317 under the label “Brown Carbon” could be itself “wavelength dependent”. The latter
318 would imply that the BrC concentration cannot be defined separately from the
319 wavelength and that its meaning is even more “operative” than in the case for the more
320 widespread OC and EC fractions. As a matter of fact, while the b_{abs}^{BrC} values discussed
321 in section 3.3, increase by a factor 5.8 moving from $\lambda = 635$ nm to $\lambda = 405$ nm, the
322 corresponding variation of the $MAC(BrC)$ values is by a factor 2.3 only. This is because
323 the BrC concentration determined at $\lambda = 405$ nm is twice the value measured at $\lambda =$
324 635 nm. The purposes and the limits of the present study prevent any firm conclusion
325 on the alternative explanation: BrC definition is wavelength dependent or the analysis
326 in red light is not sensitive enough.
- 327 • When considering the $OC_{WB}:Levo$ concentration ratio, the MWAA analysis at $\lambda = 635$
328 and $\lambda = 405$ nm give well compatible results, with a mean value of $OC_{WB}:Levo = 4.5$
329 ± 0.5 .

331 4. Conclusions

332
333 We introduced a modified version of a commercial Sunset Lab. Inc. OC/EC Analyzer. We
334 upgraded the standard instrument unit making possible the alternative use of a red ($\lambda = 635$
335 nm) or blue ($\lambda = 405$ nm) laser diode to monitor the light transmittance through the sample

336 during the thermal cycle. The analytical performance of the new set-up has been tested both
337 with artificial and real-world aerosol samples.

338 The new Sunset set-up was used to analyze a set of samples collected during mostly
339 wintertime in a mountain site of the Italian Apennines. We retrieved Brown Carbon
340 concentration values directly from the Sunset thermograms following Massabò et al., 2016.
341 Exploiting the synergic information provided by the Multi Wavelength Absorbance Analyzer,
342 MWAA (Massabò et al., 2015) we could obtain the MAC(BrC) at the two wavelengths. The
343 result at $\lambda = 635$ nm (MAC = 9.8 ± 0.4 m² g⁻¹) is in fair agreement with a previous study
344 performed for the same site in winter 2015-2016. To our knowledge, the result at $\lambda = 405$ nm,
345 MAC = 23 ± 1 m² g⁻¹ is the sole direct observation at this wavelength.

346 In our findings, the ratio between BrC and Levo concentration values depends on the
347 wavelength of the transmittance signal adopted during the thermal-optical analysis. This
348 behaviour could be due to 1) a better accuracy of the results in blue-light, more sensitive to
349 BrC, or 2) the definition of BrC itself, which has to be considered wavelength-dependent. The
350 present results do not allow any conclusive statement on this issue: actually, the label “Brown
351 Carbon”, as well as the widely used “Organic and Elemental Carbon”, comes from an operative
352 definition not without ambiguity.

353

354 **5. Acknowledgements**

355

356 This work has been partially financed by the National Institute of Nuclear Physics
357 (INFN) in the frame of the TRACCIA experiments.

358

359

360

361 **References**

362

363 Andreae, M. O. and Gelencsér, A.: Black Carbon or Brown Carbon? The nature of light-
364 absorbing carbonaceous aerosol, *Atmos. Chem. Phys.*, 6, 3131-3148, 2006.

365 Bernardoni, V., Pileci, R. E., Caponi, L., and Massabò, D.: The Multi-Wavelength Absorption
366 Analyzer (MWAA) model as a tool for source and component apportionment based on
367 aerosol absorption properties: application to samples collected in different environments,
368 *Atmosphere*, 8, 218, 2017.

369 Birch, M. E. and Cary, R. A.: Elemental carbon-based method for occupational monitoring of
370 particulate diesel exhaust: methodology and exposure issues, *Analyst*, 121, 1183–1190,
371 1996.

372 Bond, T. C. and Bergstrom, R. W.: Light absorption by carbonaceous particles: an investigative
373 review, *Aerosol Sci. Tech.*, 40, 27-67, 2006.

374 Bond, T. C. and Sun, H. L.: Can reducing black carbon emissions counteract global warming?,
375 *Environ. Sci. Technol.*, 39, 5921–5926, 2005.

376 Bond, T. C., Doherty, S. J., Fahey, D. W., Forster, P. M., Berntsen, T., De Angelo, B. J.,
377 Flanner, M. G., Ghan, S., Kärcher, B., Koch, D., Kinne, S., Kondo, Y., Quinn, P. K., Sarofim,
378 M. C., Schultz, M. G., Schulz, M., Venkataraman, C., Zhang, H., Zhang, S., Bellouin, N.,
379 Guttikunda, S. K., Hopke, P. K., Jacobson, M. Z., Kaiser, J. W., Klimont, Z., Lohmann, U.,
380 Schwarz, J. P., Shindell, D., Storelvmo, T., Warren, S. G., and Zender, C. S.: Bounding the
381 role of black carbon in the climate system: a scientific assessment, *J. Geophys. Res.-Atmos.*,
382 118, 5380-5552, 2013.

383 Bove, M. C., Brotto, P., Cassola, F., Cuccia, E., Massabò, D., Mazzino, A., Piazzalunga, A.,
384 and Prati, P.: An integrated PM_{2.5} source apportionment study: positive matrix factorisation
385 vs. the chemical transport model CAMx, *Atmos. Environ.*, 94, 274-286, 2014.

386 Cavalli, F., Putaud, J. P., Viana, M., Yttri, K. E., and Gemberg, J.: Toward a standardized
387 thermal-optical protocol for measuring atmospheric Organic and Elemental Carbon: the
388 EUSAAR protocol, *Atmos. Meas. Tech.*, 3, 79-89, 2010.

389 Chen, L. W. A., Chow, J. C., Wang, X. L., Robles, J. A., Sumlin, B. J., Lowenthal, D. H.,
390 Zimmermann, R., and Watson, J. G.: Multi-wavelength optical measurement to enhance
391 thermal-optical analysis for carbonaceous aerosol, *Atmos. Meas. Tech.*, 8, 451-461, 2015.

392 Chen, Y. and Bond, T. C.: Light absorption by organic carbon from wood combustion, *Atmos.*
393 *Chem. Phys.*, 10, 1773–1787, 2010.

394 Chow, J. C., Watson, J. G., Chen, L. W. A., Arnott, W. P., Moosmüller, H., and Fung, K. K.:
395 Equivalence of elemental carbon by thermal-optical reflectance and transmittance with
396 different temperature protocols, *Environ. Sci. Technol.*, 38, 4414-4422, 2004.

397 Chow, J. C., Watson, J. G., Mauderly, J. L., Costa, D. L., Wyzga, R. E., Vedal, S., Hidy, G.
398 M., Altshuler, S. L., Marrack, D., Heuss, J. M., Wolff, G. T., Pope, C. A. III, and Dockery,
399 D. W.: Health effects of fine particulate air pollution: lines that connect, *J. Air Waste Manag.*
400 *Assoc.*, 56, 1368–1380, 2006.

401 Chow, J. C., Watson, J. G., Chen, L. W. A., Chang, M. C. O., Robinson, N. F., Trimble, D. L.,
402 and Kohl, S. D.: The IMPROVE_A temperature protocol for thermal-optical carbon

403 analysis: maintaining consistency with a long-term database, *J. Air Waste Manag. Assoc.*,
404 57, 1014-1023, 2007.

405 Chow, J. C., Watson, J. G., Lowenthal, D. H., Chen, L. W. A., and Motallebi, N.: Black and
406 organic carbon emission inventories: review and application to California, *J. Air Waste*
407 *Manag. Assoc.*, 60, 497–507, 2010.

408 Chow, J. C., Wang, X., Sumlin, B. J., Gronstal, S. B., Chen, L. W. A., Trimble, D. L., Kohl, S.
409 D., Mayorga, S. R., Riggio, G., Hurbain, P. R., Johnson, M., Zimmermann, R., and Watson,
410 J. G.: Optical calibration and equivalence of a multiwavelength thermal-optical carbon
411 analyzer, *Aerosol Air Qual. Res.*, 15, 1145-1159, 2015.

412 Chow, J.C, Watson, J. G., Green, M. C., Wang, X., Chen, L. W. A., Trimble, D. L., Cropper,
413 P. M., Kohl S. D., and Gronstal, S. B.: Separation of brown carbon from black carbon for
414 IMPROVE and Chemical Speciation Network PM_{2.5} samples, *J. Air Waste Manag. Assoc.*,
415 68:5, 494-510, 2018.

416 Corbin J. C., Pieber S. M., Czech H., Zanatta M., Jakobi G., Massabò D., Orasche J., El
417 Haddad I., Mensah A. A., Stengel B., Drinovec L., Mocnik G., Zimmermann R., Prévôt
418 A. S. H., and M. Gysel: Brown and Black Carbon emitted by a marine engine operated on
419 heavy fuel oil and distillate fuels: optical properties, size distributions, and emission factors,
420 *J. Geophys. Res-Atmos*, 123, 6175–6195, 2018.

421 Daellenbach, K.R., Bozzetti, C., Křepelová, A., Canonaco, F., Wolf, R., Zotter, P., Fermo, P.,
422 Crippa, M., Slowik, J.G., Sosedova, Y., Zhang, Y., Huang, R. J., Poulain, L., Szidat, S.,
423 Baltensperger, U., El Haddad, I., and Prévôt, A. S. H.: Characterization and source
424 apportionment of organic aerosol using offline aerosol mass spectrometry, *Atmos. Meas.*
425 *Tech.*, 9 (1), 23-39, 2016.

426 Favez, O., El Haddad, I., Piot, C., Boreave, A., Abidi, E., Marchand, N., Jaffrezo, J. L.,
427 Besombes, J. L., Personnaz, M. B., Sciare, J., Wortham, H., Geroge, C., and D’Anna, B.:
428 Inter-comparison of source apportionment models for the estimation of wood burning
429 aerosols during wintertime in an Alpine city (Grenoble, France), *Atmos. Chem. Phys.*, 10,
430 5295-5314, 2010.

431 Feng, Y., Ramanathan, V., and Kotamarthi, V. R.: Brown carbon: a significant atmospheric
432 absorber of solar radiation?, *Atmos. Chem. Phys.*, 13, 8607-8621, 2013.

433 Ferrero, L., Močnik, G., Cogliati, S., Gregorič, A., Colombo, R., and Bolzacchini, E.: Heating
434 rate of light absorbing aerosols: time-resolved measurements, the role of clouds, and source
435 identification, *Environ. Sci. Tech.*, 52 (6), 3546-3555, 2018.

436 Filep, Á., Ajtai, T., Utry, N., Pintér, M. D., Nyilas, T., Takács, S., Máté, Z., Gelencsér, A.,
437 Hoffer, A., Schnaiter, M., Bozóki, Z., and Szabó, G.: Absorption spectrum of ambient
438 aerosol and its correlation with size distribution in specific atmospheric conditions after a
439 red mud accident, *Aerosol Air Qual. Res.*, 13, 49-59, 2013.

440 Harrison, R. M., Beddows, D. C. S., Jones A. M., Calvo A., Alves C., and Pio C.: An evaluation
441 of some issues regarding the use of aethalometers to measure woodsmoke concentrations,
442 *Atmos. Environ.*, 80, 540-548, 2013.

443 Highwood, E. J. and Kinnersley, R. P.: When smoke gets in our eyes: the multiple impacts of
444 atmospheric black carbon on climate, air quality and health, *Environ. Int.*, 32, 560–566,
445 2006.

446 Hitzenberger, R., Petzold, A., Bauer, H., Ctyroky, P., Pouresmaeil, P., Laskus, L., and
447 Puxbaum, H.: Intercomparison of thermal and optical measurement methods for elemental
448 carbon and black carbon at an urban location, *Environ. Sci. Technol.*, 40 (20), 6377-6383,
449 2006.

450 Karanasiou, A., Minguillon, M. C., Viana, M., Alaustey, A., Puaud, J. P., Maenhaut, W.,
451 Panteliadis, P., Močnik, G., Favez, O., and Kuhlbusch, T. A.: Thermal-optical analysis for
452 the measurement of elemental carbon (EC) and organic carbon (OC) in ambient air, a
453 literature review, *Atmos. Meas. Tech. Discuss.*, 8, 9649-9712, 2015.

454 Kirchstetter, T. W., Novakok, T., and Hobbs, P. V.: Evidence that the spectral dependence of
455 light absorption by aerosols is affected by organic carbon, *J. Geophys. Res.*, 109, D21208,
456 2004.

457 Lack, D. A. and Langridge, J. M.: On the attribution of black and brown carbon light absorption
458 using the Ångström exponent, *Atmos. Chem. Phys.*, 13, 10535-10543, 2013.

459 Lack, D. A., Langridge, J. M., Bahreini, R., Cappa, C. D., Middlebrook, A. M., and Schwarz,
460 J. P.: Brown carbon and internal mixing in biomass burning particles, *Proc. Natl. Acad. Sci.*,
461 109, 14802-14807, 2012.

462 Laskin, A., Laskin, J., and Nizkorodov S. A.: Chemistry of atmospheric brown carbon, *Chem.*
463 *Rev.*, 115 (10), 4335–4382, 2015.

464 Lewis, K., Arnott, W. P., Moosmüller, H., and Wold, C. E.: Strong spectral variation of
465 biomass smoke light absorption and single scattering albedo observed with a novel dual-
466 wavelength photoacoustic instrument, *J. Geophys. Res.*, 113, D16203, 2008.

467 Massabò, D., Bernardoni, V., Bove, M. C., Brunengo, A., Cuccia, E., Piazzalunga, A., Prati,
468 P., Valli, G., and Vecchi, R.: A multi-wavelength optical set-up for the characterization of
469 carbonaceous particulate matter, *J. Aerosol Sci.*, 60, 34-46, 2013.

470 Massabò, D., Caponi, L., Bernardoni, V., Bove, M. C., Brotto, P., Calzolari, G., Cassola, F.,
471 Chiari, M., Fedi, M. E., Fermo, P., Giannoni, M., Lucarelli, F., Nava, S., Piazzalunga, A.,
472 Valli, G., Vecchi, R., and Prati, P.: Multi-wavelength optical determination of black and
473 brown carbon in atmospheric aerosols, *Atmos. Environ.*, 108, 1-12, 2015.

474 Massabò, D., Caponi, L., Bove, M. C., and Prati, P.: Brown carbon and thermal-optical
475 analysis: a correction based on optical multi-wavelength apportionment of atmospheric
476 aerosols, *Atmos. Environ.*, 125, 119-125, 2016.

477 Mauderly, J. L. and Chow, J. C.: Health effects of organic aerosols, *Inhal. Toxicol.*, 20, 257–
478 288, 2008.

479 Moosmüller, H., Chakrabarty, R. K., and Arnott, W. P.: Aerosol light absorption and its
480 measurement: a review, *J. Quant. Spectrosc. Ra.*, 110, 844-878, 2009.

481 Moosmüller, H., Chakrabarty, R. K., Ehlers, K. M., and Arnott, W. P.: Absorption Ångström
482 coefficient, brown carbon, and aerosols: basic concepts, bulk matter, and spherical particles,
483 *Atmos. Chem. Phys.*, 11, 1217-1225, 2011.

484 Olson, M. R., Garcia, M. V., Robinson, M. A., Van Rooy, P., Dietenberger, M. A., Bergin, M.,
485 and Schauer, J. J.: Investigation of black and brown carbon multiple-wavelength-dependent
486 light absorption from biomass and fossil fuel combustion source emissions, *J. Geophys. Res.*
487 *Atmos.*, 120, 2015.

488 Panteliadis, P., Hafkenscheid, T., Cary, B., Diapouli, E., Fischer, A., Favez, O., Quincey, P.,
489 Viana, M., Hitzengerger, R., Vecchi, R., Saraga, D., Sciare, J., Jaffrezo, J. L., John, A.,
490 Schwarz, J., Giannoni, M., Novak, J., Karanasiou, A., Fermo, P., and Maenhaut, W.: ECOC
491 comparison exercise with identical thermal protocols after temperature offset correction –
492 instrument diagnostics by in-depth evaluation of operational parameters, *Atmos. Meas.*
493 *Tech.*, 8, 779–792, 2015.

494 Piazzalunga, A., Fermo, P., Bernardoni, V., Vecchi, R., Valli, G., and De Gregorio M. A.: A
495 simplified method for levoglucosan quantification in wintertime atmospheric particulate
496 matter by high performance anion-exchange chromatography coupled with pulsed
497 amperometric detection, *Int. J. Environ. An. Ch.*, 90, 934-947, 2010.

498 Piazzalunga, P., Bernardoni, V., Fermo, P., Valli, G., and Vecchi, R.: On the effect of water-
499 soluble compounds removal on EC quantification by TOT analysis in urban aerosol samples,
500 *Atmos. Chem. Phys.*, 11, 10193-10203, 2011.

501 Pope, C. A. III and Dockery, D. W.: Health effects of fine particulate air pollution: lines that
502 connect, *J. Air Waste Manag. Assoc.*, 56, 709–742, 2006.

503 Pöschl, U.: Aerosol particle analysis: challenges and progress, *Anal. Bioanal. Chem.*, 375,
504 3032, 2003.

505 Sandradewi, J., Prevot, A. H., Szidat, S., Perron, N., Rami Alfarra, M., Lanz, V., Weingartner,
506 E., and Baltensperger, U.: Using aerosol light absorption measurements for the quantitative
507 determination of wood burning and traffic emission contributions to particulate matter,
508 *Environ. Sci. Technol.*, 3316-3323, 2008.

509 Subramanian, R., Khlystov, A. Y., and Robinson, A. L.: Effect of peak inert-mode temperature
510 on elemental carbon measured using thermal-optical analysis, *Aerosol Sci. Tech.*, 40, 763–
511 780, 2006.

512 Utry, N., Ajtai, T., Filep, Á., Dániel P. M., Hoffer, A., Bozoki, Z., and Szabó, G.: Mass specific
513 optical absorption coefficient of HULIS aerosol measured by a four-wavelength
514 photoacoustic spectrometer at NIR, VIS and UV wavelengths, *Atmos. Environ.*, 69, 321-
515 324, 2013.

516 Utry, N., Ajtai, T., Filep, Á., Pintér, M., Török, Zs., Bozóki, Z., and Szabó, G.: Correlations
517 between absorption Angström exponent (AAE) of wintertime ambient urban aerosol and its
518 physical and chemical properties, *Atmos. Environ.*, 91, 52-59, 2014.

519 Vassura, I., Venturini, E., Marchetti, S., Piazzalunga, A., Bernardi, E., Fermo, P., and Passarini,
520 F.: Markers and influence of open biomass burning on atmospheric particulate size and
521 composition during a major bonfire event, *Atmos. Environ.*, 82, pp. 218-225, 2014.

522 Watson, J. G., Chow, J. C., and Chen, L. W. A.: Summary of organic and elemental
523 carbon/black carbon analysis methods and intercomparisons, *Aerosol Air Qual. Res.*, 5, 65-
524 102, 2005.

525 Yang, H. and Yu, J. Z.: Uncertainties in charring correction in the analysis of elemental and
526 organic carbon in atmospheric particles by thermal-optical methods, *Environ. Sci. Technol.*,
527 36, 5199-5204, 2002.

528 Yang, M., Howell, S. G., Zhuang, J., and Huebert, B. J.: Attribution of aerosol light absorption
529 to black carbon, brown carbon, and dust in China - interpretations of atmospheric
530 measurements during EAST-AIRE, *Atmos. Chem. Phys.*, 9, 2035-2050, 2009.

531 Zheng, G., He, K., Duan, F., Cheng, Y., and Ma, Y.: Measurement of humic-like substances in
532 aerosols: A review, *Environ. Pollut.*, 181, 301-314, 2013.

533 Zhi, G., Chen, Y., Sheng, G., and Fu, J.: Effects of temperature parameters on thermal-optical
534 analysis of organic and elemental carbon in aerosol, *Environ. Monit. Assess.*, 154, 253–
535 261, 2008.

FIGURE CAPTIONS

536
537
538
539
540
541
542
543
544
545
546
547
548
549
550
551
552
553
554
555
556
557
558
559
560
561
562
563
564
565

Figure 1: The new $\lambda = 405$ nm laser diode mounted by a steel adapter on the SUNSET furnace (top) and comparison with the standard $\lambda = 635$ nm laser diode implemented by the manufacturer (bottom).

Figure 2: Quantification of TC and EC at $\lambda = 635$ nm (red) and $\lambda = 405$ nm (blue) for the set of synthetic Aquadag samples. Top: NIOSH5040 protocol, bottom: EUSAAR_2 protocol.

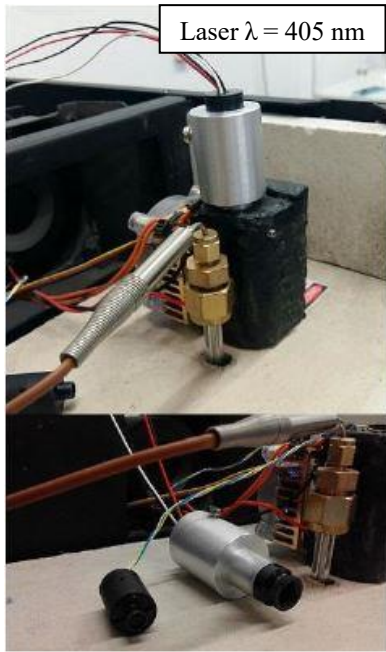
Figure 3: Quantification of TC and EC at $\lambda = 635$ nm (red) and $\lambda = 405$ nm (blue) for the set of synthetic Aquadag + Ammonium Sulphate samples by the EUSAAR_2 protocol.

Figure 4: EC concentration measured in two sub-sets of PM10 samples collected in consecutive days in the urban area of Genoa in late spring 2016. Values determined with the Sunset analyzer equipped with blue and red laser diodes, are compared.

Figure 5: Primary axis: Optical apportionment of the aerosol absorption coefficient (b_{abs}) at $\lambda = 635$ nm (top) and $\lambda = 405$ nm (bottom). Secondary axis: experimental AAE (AAE_{exp}) values obtained by fitting the measured b_{abs} values with a power-law relationship $b_{\text{abs}}(\lambda) \sim \lambda^{-\text{AAE}}$. FF and WB stand for Fossil Fuel and Wood Burning, respectively.

Figure 6: Aerosol absorption coefficient apportioned to Brown Carbon ($b_{\text{abs}}^{\text{BrC}}$) at $\lambda = 635$ nm (top) and at $\lambda = 405$ nm (bottom) vs. levoglucosan concentration.

Figure 7: Comparison between the aerosol absorption coefficient apportioned to Brown Carbon vs. the resulting operative BrC concentration values at $\lambda = 635$ nm (top) and at $\lambda = 405$ nm (bottom).



566

567 Figure 1

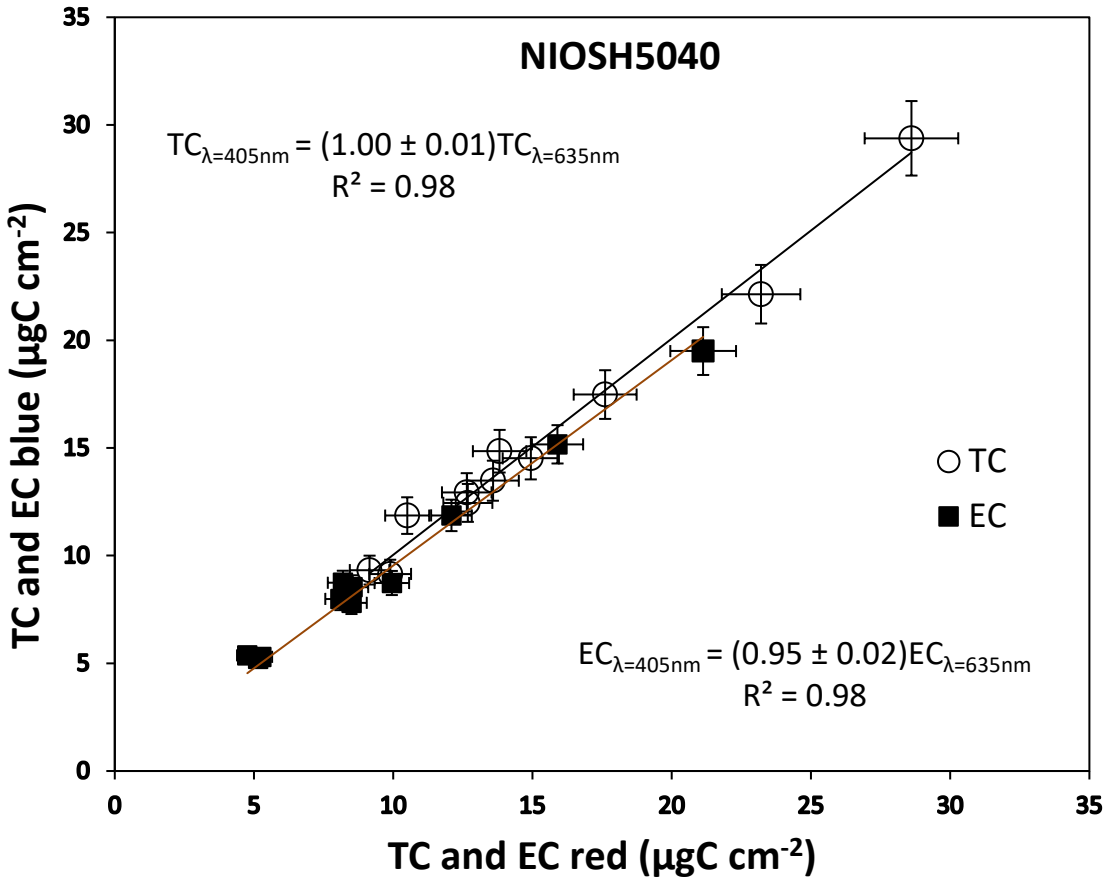
568

569

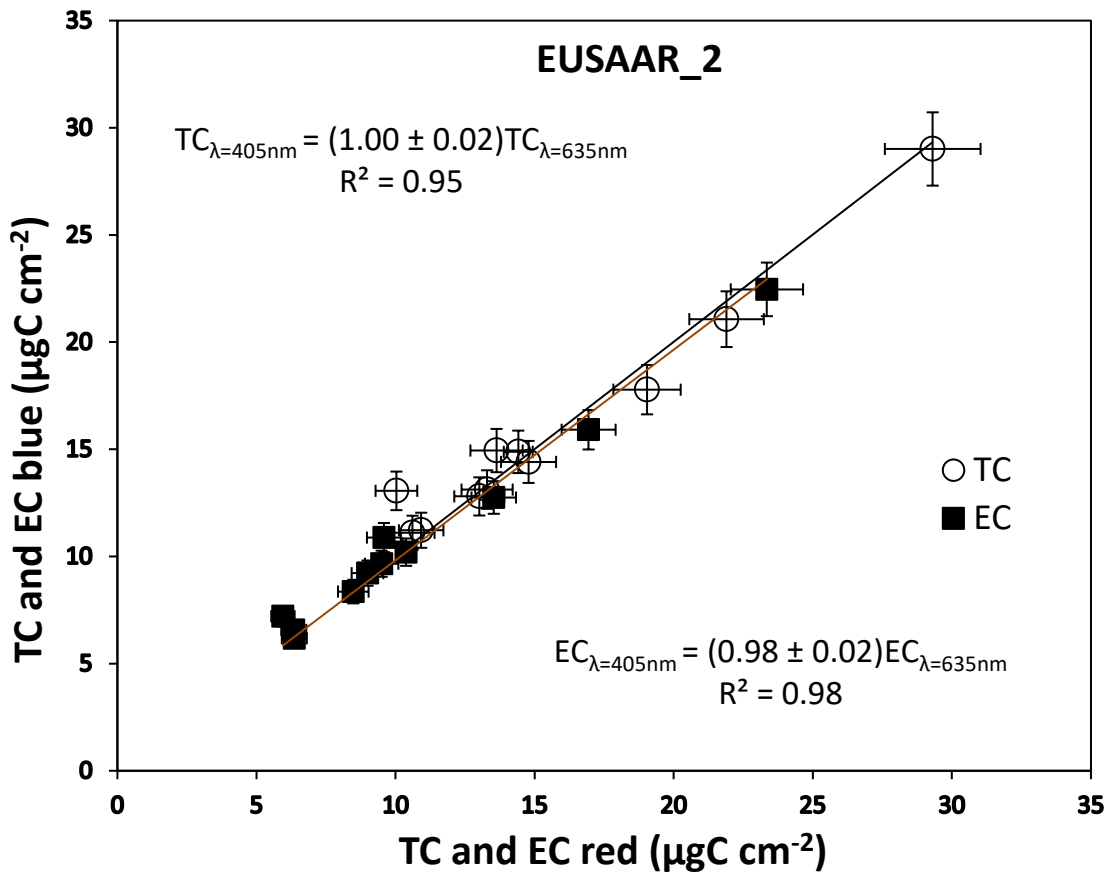
570

571

572



573

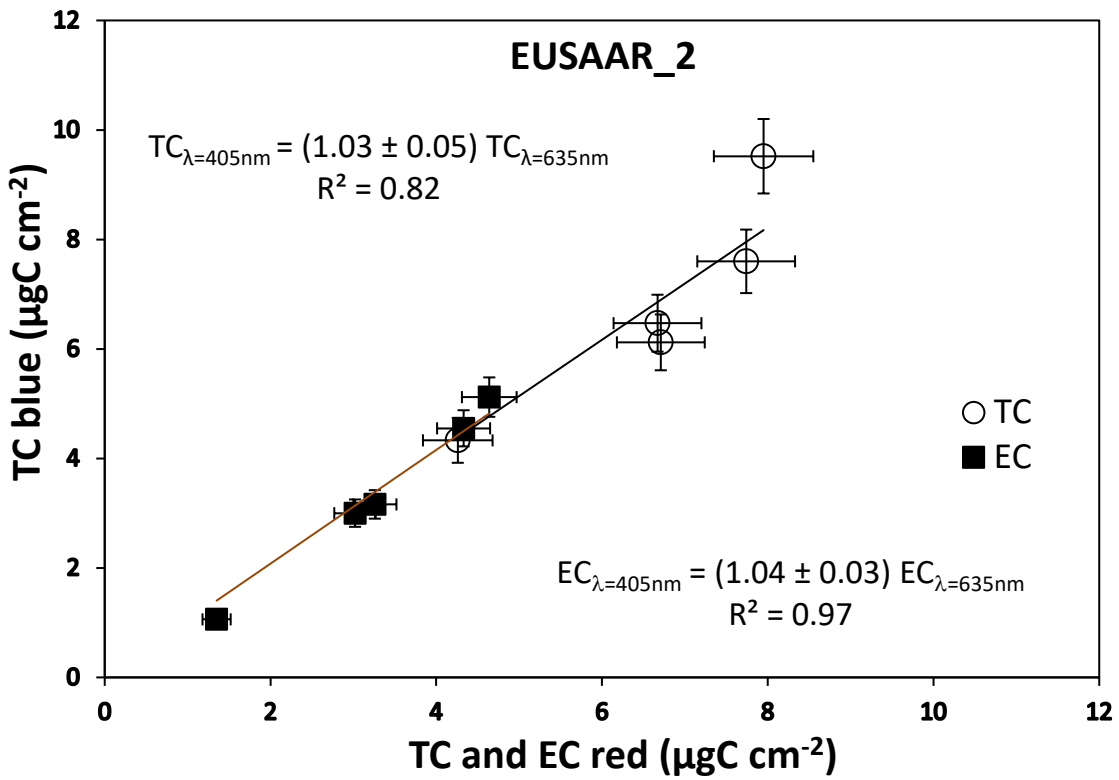


574

575

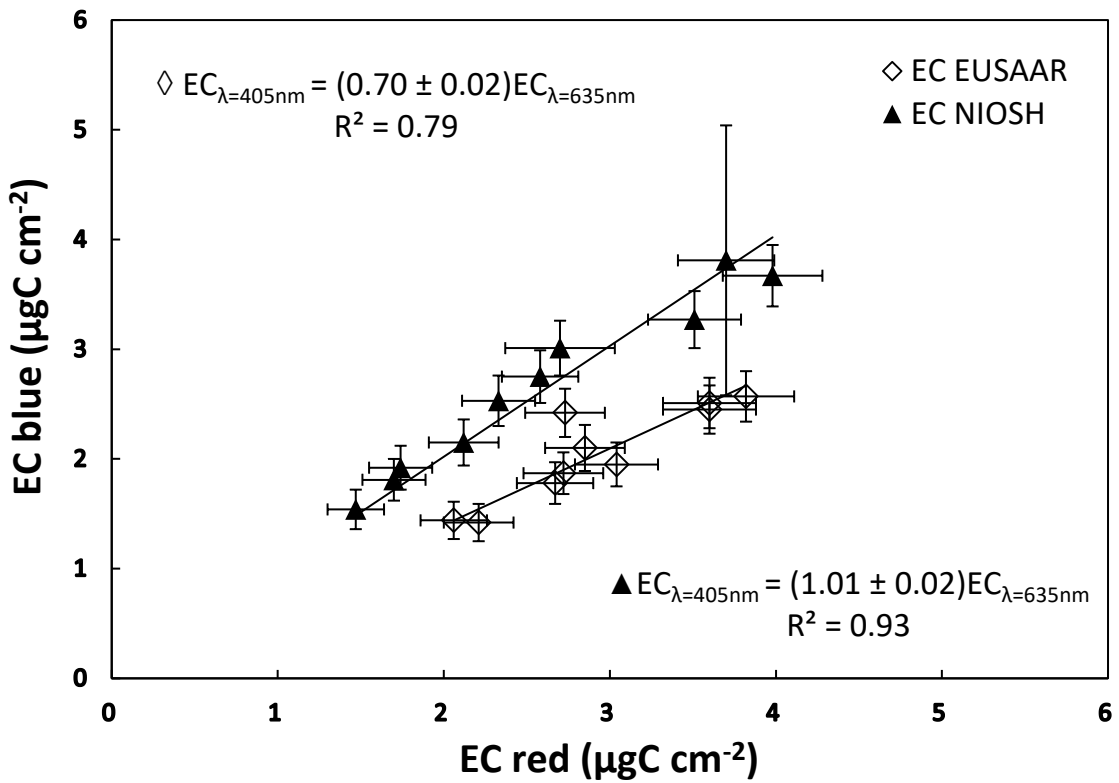
Figure 2

576



577
578

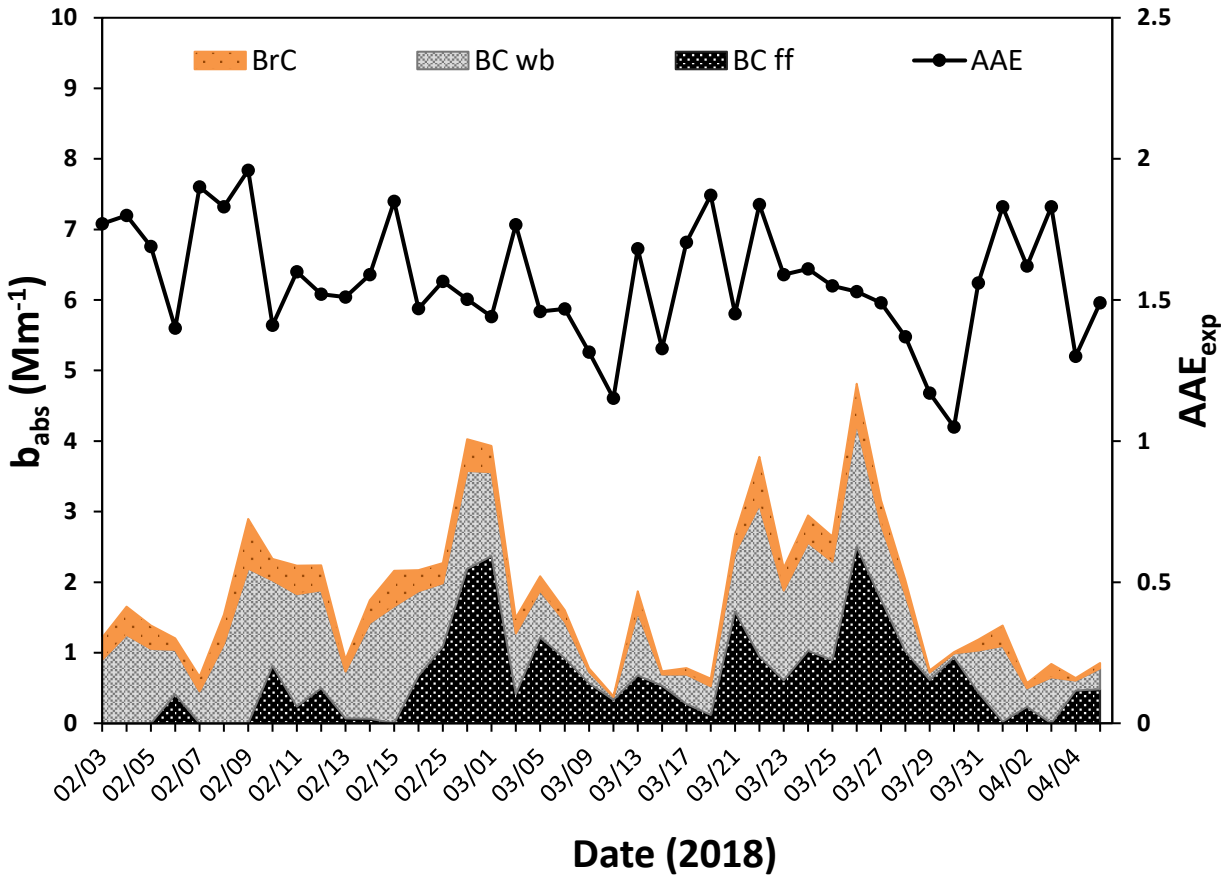
Figure 3



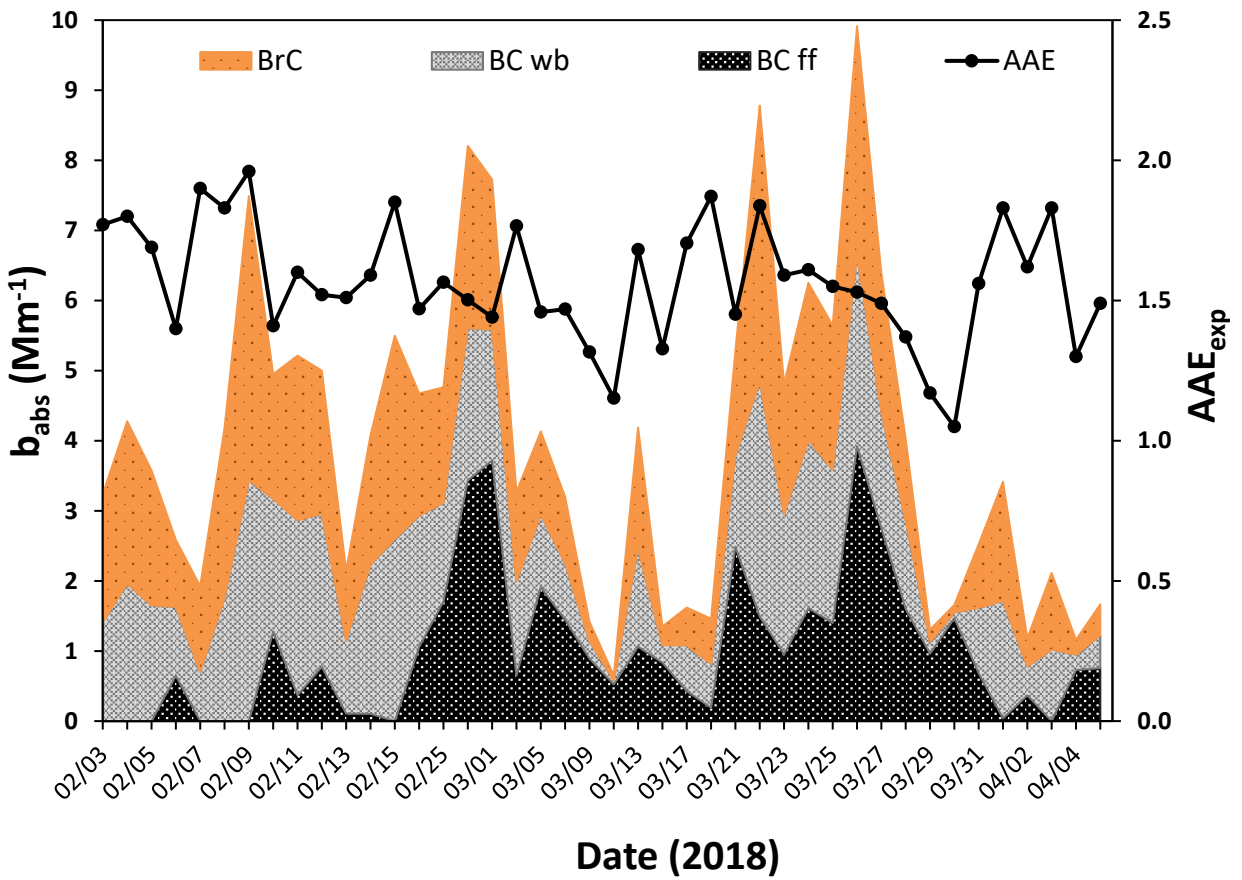
579
580

Figure 4

581



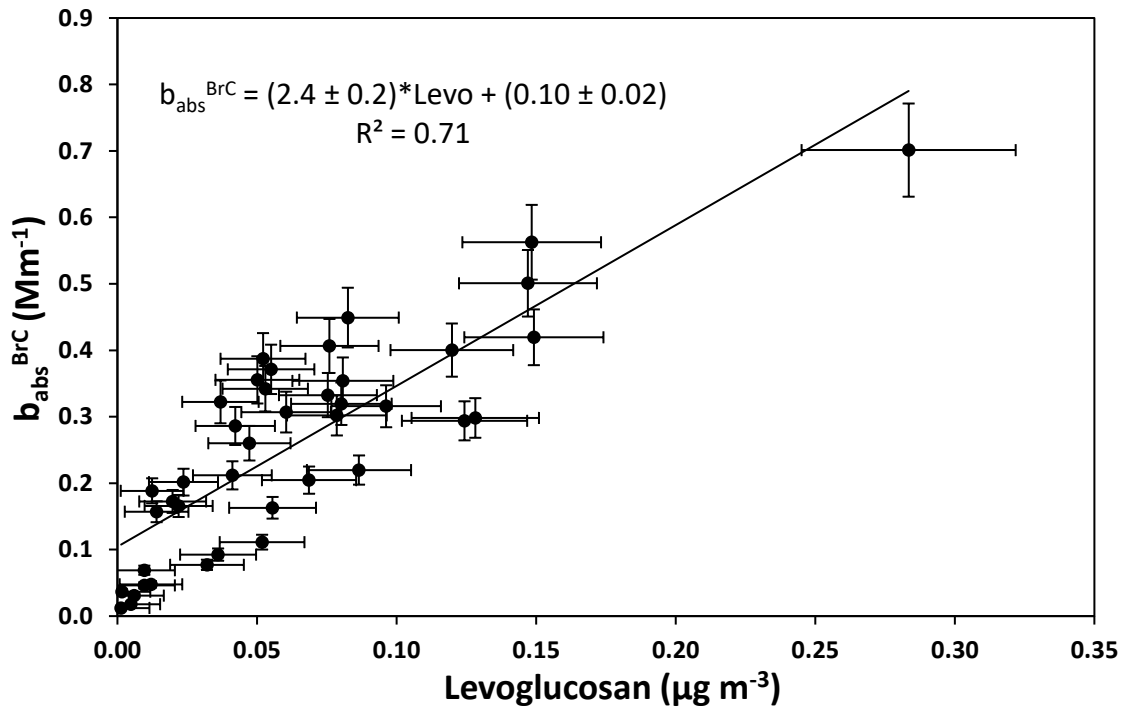
582



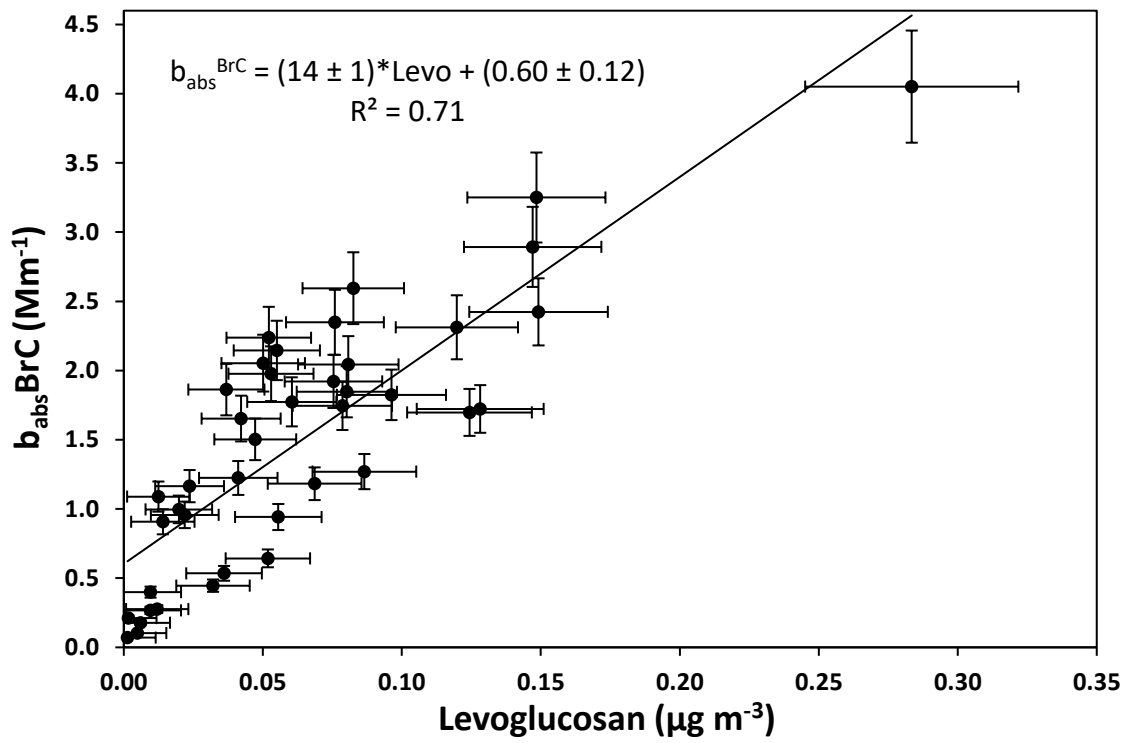
583

584

Figure 5

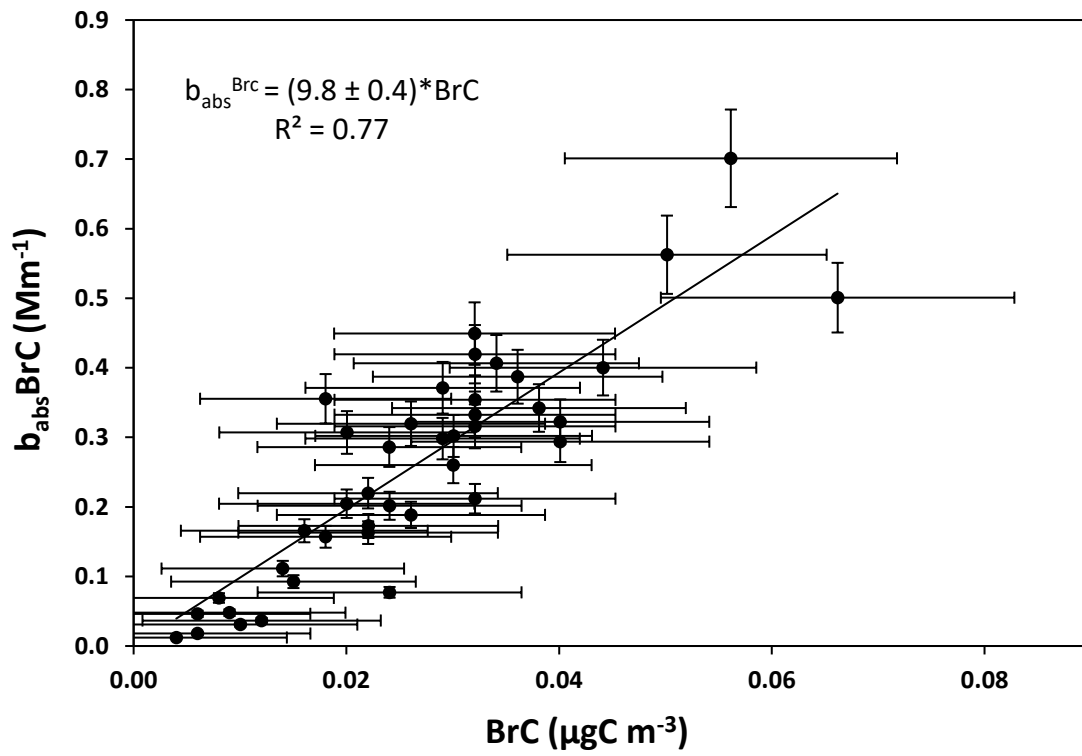


585
586
587

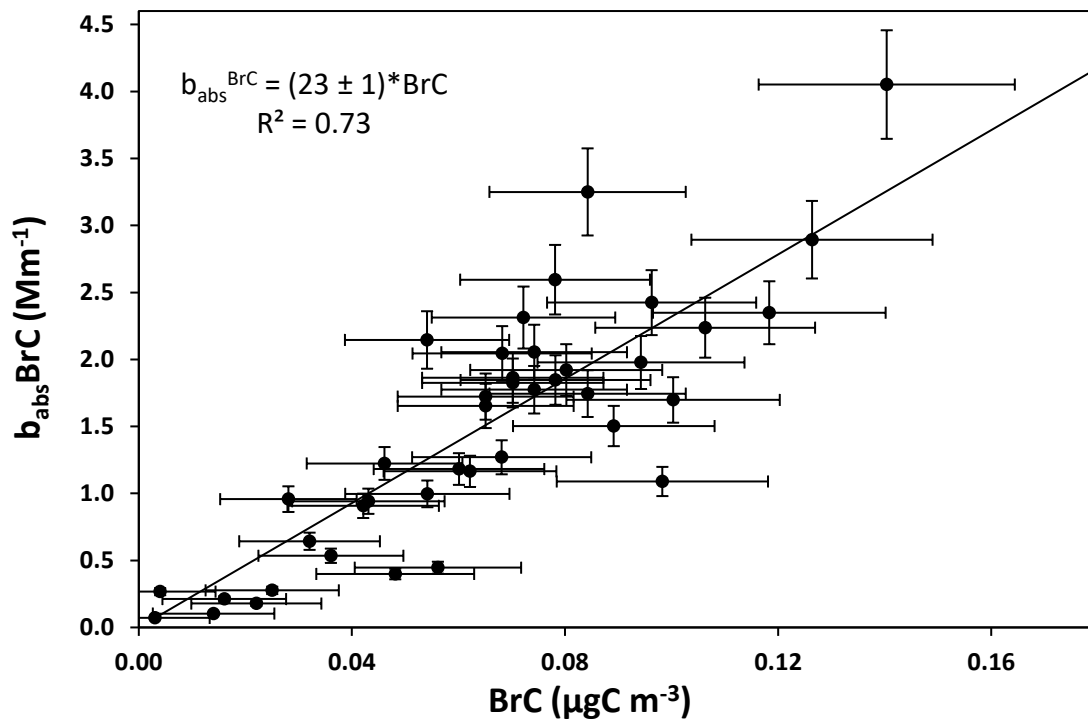


588
589

Figure 6



590
591



592
593

Figure 7